



## Domain wall resistance in epitaxial Fe wires

C. Hassel<sup>a,\*</sup>, F.M. Römer<sup>a</sup>, N. Reckers<sup>a</sup>, F. Kronast<sup>b</sup>, G. Dumpich<sup>a</sup>, J. Lindner<sup>a</sup>

<sup>a</sup> Fachbereich Physik and Center for Nanointegration Duisburg-Essen (CeNIDE), Universität Duisburg-Essen, 47048 Duisburg, Germany

<sup>b</sup> Bessy GmbH, Berlin, Germany

### ARTICLE INFO

#### Article history:

Received 11 August 2010

Received in revised form

5 December 2010

Available online 10 December 2010

#### Keywords:

Domain wall

Electronic transport

Domain wall resistance

### ABSTRACT

We studied the magnetoresistance behavior of epitaxial Fe wires grown on GaAs(1 1 0) with varying widths at room temperature. Single nanowires show a wire width ( $w$ ) dependence of the coercive field, which increases with  $1/w$  for decreasing wire widths. This enables the pinning of a single domain wall in the connection area of two wires with different widths. Magnetoresistance measurements of such wire structures clearly reveal resistance contributions arising from a domain wall. The presence of the domain wall is proven by photoemission electron-microscopy with synchrotron radiation. Moreover, micromagnetic simulations are performed to determine the spin orientations, especially within the domain wall. This permits us to calculate the anisotropic magnetoresistance caused by the domain wall. Taking this into account, we determine the intrinsic domain wall resistance, for which we found a positive value of 0.2%, in agreement with theoretical predictions.

© 2010 Elsevier B.V. All rights reserved.

### 1. Introduction

Domain walls have attracted much interest in the last years, also due to the fact that storage devices based on domain walls have been suggested [1]. Beside the studies of current-induced domain wall motion [2], theory and experiment have made great efforts to determine the intrinsic resistance of domain walls. A review to the topic of the domain wall resistance can be found in [3]. Levy et al. have calculated a *positive* contribution of a domain wall to the resistance based on a Giant magnetoresistance (GMR)-like approach, where spin mixing between the minority and majority electrons is considered [4]. In contrast, Tatara et al. predict a *negative* contribution taking into account that due to a presence of the domain wall the coherence of electron waves is disturbed [5]. The experimental determination of the domain wall resistance in out-of-plane magnetized materials can be performed in a straightforward manner, since contributions from the anisotropic magnetoresistance (AMR) [6] can be neglected inside the occurring Bloch walls [7,8] for this geometry. However, for in-plane magnetized materials, the rotation of the magnetization inside the domain wall causes a contribution from the AMR, which has to be considered for the determination of the intrinsic domain wall resistance [9]. Ruediger et al. find a negative contribution of the intrinsic domain wall resistance by measuring at the so-called compensation temperature, where AMR and Lorentz magnetoresistance cancel out [10]. However, also positive contributions to the domain wall resistance were found for in-plane magnetized systems [11].

In the present paper we report on magnetoresistance measurements on epitaxial Fe wires grown on GaAs(1 1 0). The resistance change due to the presence of a single domain wall is measured. The contributions from the AMR are taken into account by micromagnetic simulations using the OOMMF code [12]. Thus, it is possible to determine the intrinsic domain wall resistance for this in-plane magnetized material.

### 2. Experimental details

We have prepared epitaxial Fe(1 1 0) films with a thickness of 10 nm on Si-doped GaAs(1 1 0) substrates capped with Ag and Pt to prevent oxidation within an ultrahigh vacuum (UHV) chamber with a base pressure of  $p < 1 \times 10^{-10}$  mbar. The films are structured into wires by a process consisting of electron beam lithography (EBL) and Ar<sup>+</sup> ion sputtering. The wires are contacted in a second EBL step with gold wires, which enables us to carry out four-point resistance measurements. Details of the fabrication process can be found in [13,14]. The anisotropy constants of the film were determined using ferromagnetic resonance at room temperature [14]. The magnetocrystalline anisotropies of the film which was used to prepare the wires described in this paper are  $k_{211} = 4.0 \times 10^4$  J/m<sup>3</sup> and  $k_4 = 3.2 \times 10^4$  J/m<sup>3</sup> for the in-plane uniaxial and the cubic anisotropy, respectively, as determined with ferromagnetic resonance (FMR). Both easy axes are oriented parallel to the [0 0 1] direction, so that the resulting anisotropy is larger than that known for bulk iron. Since we use substrates with a (1 1 0) surface, the in-plane direction, which is aligned perpendicular to the [0 0 1] direction, is an intermediate  $[\bar{1} 1 0]$  direction.

\* Corresponding author.

E-mail address: [christoph.hassel@uni-due.de](mailto:christoph.hassel@uni-due.de) (C. Hassel).

This causes an increase of the anisotropy of longitudinal magnetized wires as compared to Fe(0 0 1).

Magnetoresistance measurements are carried out using a self-built AC-resistance bridge at room temperature. Measurement currents are in the range of 10  $\mu\text{A}$  to avoid heating effects as well as current-induced domain wall depinning. The sample is inside an evacuated sample tube to exclude thermal fluctuations. The system is equipped with an electromagnet supplying magnetic fields up to  $\pm 2$  T.

Magnetic imaging is performed at the Bessy beamline UE49 using a commercial Photoemission electron-microscope with the synchrotron radiation fixed at the energy of the Fe  $L_3$  edge (XPEEM) [15]. Magnetic contrast is achieved taking the differences of images with different helicities of the incoming light using the XMCD effect [16]. Since it is possible to tilt the sample with respect to the incoming light direction, longitudinal as well as transversal magnetization of the wires could be imaged.

### 3. Results and discussion

It is well known that the coercive field of longitudinally magnetized polycrystalline wires depends strongly on the width  $w$  of the wires [17,18]. Fig. 1 shows the coercive fields obtained for the epitaxial Fe wires investigated in this paper. All wires are oriented parallel to the easy [0 0 1]-direction, where also the external magnetic field is applied (see inset in Fig. 1). For the determination of the coercive fields, we used magnetoresistance measurements at room temperature. The solid line is a fit according to a  $1/w$  function, which is usually used in literature to describe the increase of coercivity [17,18]. One can clearly see that the coercive fields increase with decreasing wire widths and that the  $1/w$  function agrees well with our data points.

Using this wire width dependence, it is possible to create artificial pinning centers by varying the wire width of a wire [19]. Fig. 2 shows a magnetoresistance measurement of a wire consisting of two parts, which have different widths. The broad part has a width of 1750 nm, while the smaller part has a width of 280 nm. The resistance is measured for a  $2.5 \mu\text{m}$  wide area at the intersection of these two wires. The external field is applied parallel to the long wire axis. Starting from saturation, one observes a linear increase of the resistance when reducing the external field. This increase continues by applying small magnetic fields in the other direction. At a field of  $B_{c,1} \approx 17$  mT, we observe a sharp resistance

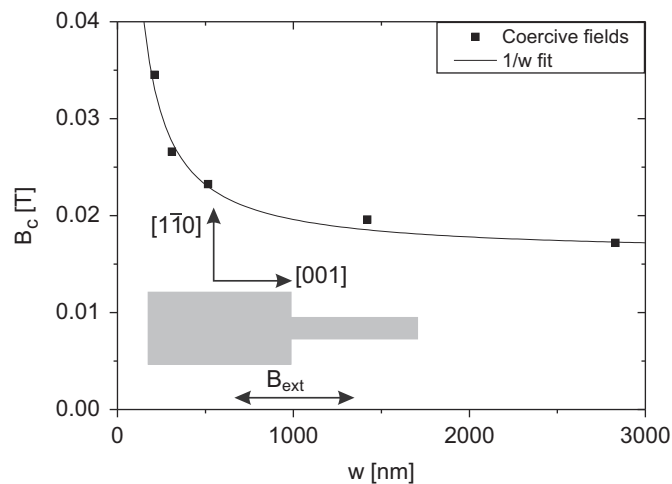


Fig. 1. Wire width dependence of the coercive field of single epitaxial Fe wires, which are oriented parallel to the [0 0 1]-direction. A sketch of these orientation is shown in the inset. The coercive fields were determined by magnetoresistance measurements at room temperature.

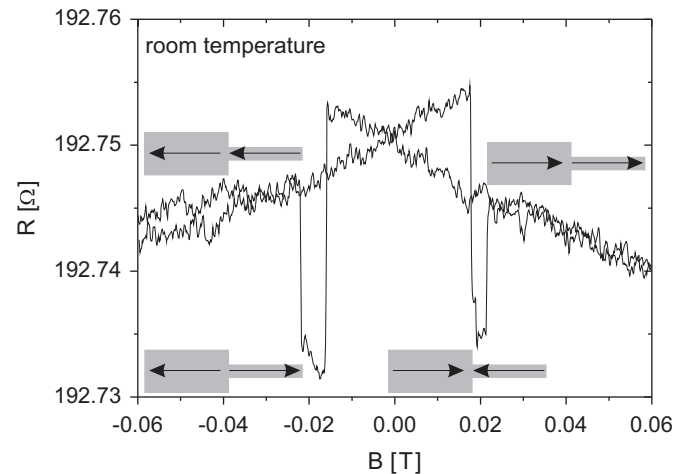


Fig. 2. Magnetoresistance measurement at room temperature of a structure consisting of two wires with different widths as also sketched in the insets. Clearly observable are resistance jumps which are attributed to the pinning and depinning of the domain wall in the junction area.

jump downwards, which is followed by a sharp resistance jump upwards at a field of  $B_{c,2} \approx 22$  mT. By further increasing the magnetic field, a linear decrease of the resistance is observed.

The linear resistance behavior with magnetic field can be explained by electron–magnon scattering [20], which gives a linear dependence of the resistance with varying magnetic fields. The observed slope of our curves agrees well with the data from Ref. [20]. The resistance jump downwards occurs at the coercive field of the broader wire. The field  $B_{c,1}$  for the jump to occur agrees well with the one obtained for the single wires as shown in Fig. 1 (18 mT). For  $B_{c,1} < B < B_{c,2}$  a single domain wall is pinned in the constriction area between the two wire parts. At  $B_{c,2}$  the smaller wire is reversed and the domain wall is removed from the constriction area. Note that in this case  $B_{c,2}$  is considerably smaller than the coercive field of the single wire (29 mT), which can be attributed to the fact that a domain wall has already been nucleated in the broad wire and thus the reversal field is determined by depinning rather than nucleation. The resistance jump downwards at  $B_{c,1}$  and the jump upwards at  $B_{c,2}$  do not have the same amplitude, since the contribution from the electron–magnon scattering is added to the domain wall resistance for the jump downwards and subtracted for the jump downwards. Averaging of the two resistance jumps leads to an overall negative resistance contribution of  $(\Delta R/R) = -0.8 \times 10^{-4}$ . From that one might conclude that the intrinsic contribution of a single domain wall to the resistance is negative. However, this overall resistance change consists of contributions due to the AMR [6] as well as the intrinsic the domain wall resistance. The contribution of the AMR is—due to the rotation of the magnetization inside the domain wall—negative. To consider this contribution quantitatively, we performed imaging with XPEEM and micromagnetic simulations.

Fig. 3 shows XPEEM images of a wire structure as measured in Fig. 2, whereby the geometry of the structure is indicated by the dashed lines. The Au contacts which are oriented perpendicular to the wire axis, are visible as grey contrast. Fig. 3a shows the magnetization component parallel to the long wire axis and Fig. 3b shows the magnetization component transversal to the long wire axis. Prior to these images, a small magnetic field of 20 mT was applied to the wire along [0 0 1] direction, after it was saturated along [0 0  $\bar{1}$ ]. For Fig. 3a the synchrotron radiation was coming from the left side. Since the gold contacts are placed on top of the Fe wire, no contrast from the Fe wire below the Au contact is visible. Additionally, the gold edges produce a shadow effect as

Download English Version:

<https://daneshyari.com/en/article/10710203>

Download Persian Version:

<https://daneshyari.com/article/10710203>

[Daneshyari.com](https://daneshyari.com)